CBPF

Notas de Física

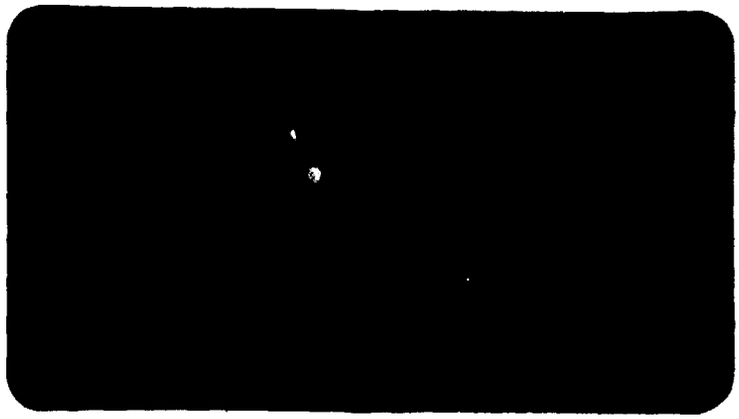

NOTAS DE FÍSICA é uma pré-publicação de trabalhos em Física do CBPF

NOTAS DE FÍSICA is a series of preprints from CBPF

Pedidos de cópias desta publicação devem ser enviados aos autores ou à:

Requests for free copies of these reports should be addressed to:

Divisão de Publicações do CBPF-CNPq
Rua Dr. Xavier Sigaud, 150
22.290 - Rio de Janeiro - RJ.
Brasil

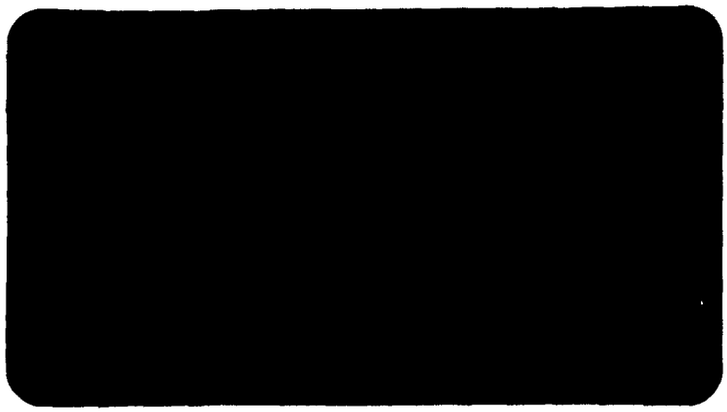

Secretaria de Planejamento da Presidência da República
CNPq - Conselho Nacional de Desenvolvimento Científico e Tecnológico
CBPF - Centro Brasileiro de Pesquisas Físicas
Rio de Janeiro, RJ
BRASIL

CBPF-NF-016/83

ELECTRIC FIELD GRADIENT AND ELECTRONIC STRUCTURE OF LINEAR-BONDED HALIDE COMPOUNDS*

by

D.E. Ellis[1], D. Guenzburger and
H.B. Jansen[2]

Centro Brasileiro de Pesquisas Físicas - CNPq
Rua Xavier Sigaud, 150
22290 Rio de Janeiro, RJ - BRASIL

[1]Department of Physics and Astronomy
Nothwestern University
Evanston, Illinois 60201 - U.S.A.

[2]Department of Chemistry
The Free University
Amsterdam, NETHERLANDS

Electric Field Gradient and Electronic Structure of Linear-Bonded Halide Compounds*

D.E. Ellis, Department of Physics and Astronomy, Northwestern University, Evanston, Illinois 60201

Diana Guenzburger, Centro Brasileiro de Pesquisas Fisicas, Rio de Janeiro, Brazil.

H.B. Jansen, Department of Chemistry, The Free University, Amsterdam, The Netherlands.

Abstract

The importance of covalent metal-ligand interactions in determining hyperfine fields and energy-level structure of MX_2 linear-bonded halide compounds has been studied, using the self-consistent local density molecular orbital approach. ~~We present~~ Results for $FeCl_2$, $FeBr_2$ and $EuCl_2$ obtained are preliminary using the Discrete Variational Method with numerical basis sets. The high spin configuration for the iron compounds, first predicted by Berkowitz, et al., is verified; a successful comparison with gas phase photoelectron spectra is made. Variation of the predicted electric field gradient with bond length R is found to be rapid; the need for an EXAFS measurement of R for the matrix isolated species and experimental determination of the sign of the EFG is seen to be crucial for more accurate determinations of the ^{57}Fe quadrupole moment.

I. INTRODUCTION

Electric and magnetic hyperfine fields have long been used to characterize the electronic density in the vicinity of a resonant nucleus. Despite the large number of experimental studies which clearly establish empirical relations and trends, theoretical advances have been rather slow. There are several reasons for the slow development of adequate theories for interpreting hyperfine data. First, the simplified models of one-electron phenomena fail since shielding and other relaxation effects are found to be important. In the multicenter molecular or solid state environment, this means that arduous self-consistent field calculations have to be performed, at the least. Experience with atomic data and applications of many-body theory have shown that in some cases complex configuration mixing effects have to be evoked. Second, the hyperfine interactions measure multipolar moments of the electronic charge or spin density which are not directly related to the total energy of the system. Thus, schemes which seek to optimize the wavefunction with respect to energy, can result in very great uncertainties in predicted hyperfine parameters. The literature of the last twenty years of Hartree-Fock calculations on molecules reveals the uncertainties due to limited basis sets and computational procedures. Nevertheless, as the quality of computational efforts has improved, it is possible to hope that the hyperfine parameters have become better determined, at least in principle. Finally, because of these aforementioned difficulties, theoretical efforts in recent years have been rather meager.

In studying the electronic structure of solid state and complex molecular systems, the self-consistent local density theories have proved to be both capable of implementation and capable of providing quantitative data for both spectroscopic and density-derived properties[1-3]. Quite a number of solid

state investigations have been made, using either the Kohn-Sham-Slater models,[1,4] or more sophisticated exchange-correlation schemes, particularly for metals. The use of hyperfine fields as probes of defects and impurity structures in metals is currently one of the most valuable applications of hyperfine techniques. However, it is possible to wonder how secure the foundations of the hyperfine results are.

In this paper we consider some relatively simple linear bonded MX_2 metal halide systems which have been suggested as "calibration points"[5-9]. In principle, one hopes not only to establish the limits of validity of the theory, as applied for example to transition metal and rare earth compounds, but also to help determine the nuclear properties such as change in radius upon excitation $\langle \Delta r^2 \rangle$ and the quadrupole moment Q. In order to complete our calibration and to compare with data available from other first-principles methods, we also discuss results for the simple gas phase molecules HCl and Cl_2.

In Section II we briefly sketch the underlying one-electron theory and the variational method used to solve the self-consistent field equations. The diatomic molecule results are discussed in Section III, and rough error bounds for the theory are thus established. Our data for $FeCl_2$ and $FeBr_2$ are presented in Section IV, and compared with gas-phase photoelectron data and electric field gradient studies on matrix-isolated species. Some preliminary results for $EuCl_2$ are given in Section V.

II. THEORETICAL APPROACH

A. One-Electron Model

The self-consistent one-electron local density (LD) theory has been used increasingly in studying the structure of molecules, as an alternative to the more traditional ab initio methods. The LD theory, as developed by Slater, Kohn, Sham and others[1-4] is the most successful model available for the description of electronic structure of solids. In both molecules and solids one iteratively solves the Schrödinger equation.

$$(h_\sigma - \epsilon_{n\sigma})\,\psi_{n\sigma}(\vec{r}) = 0 \qquad (1)$$

to determine self-consistently energy levels, wavefunctions, and charge and spin density ρ_σ:

$$\rho_\sigma = \sum_n f_{n\sigma} |\psi_{n\sigma}|^2 \qquad (2)$$

The single particle hamiltonian is itself a functional of the densities,

$$h_\sigma = t + V_{Coul}(\rho) + V_{xc,\sigma}(\rho) \qquad (3)$$

where t is the kinetic energy operator, V_{Coul} is the electrostatic Coulomb potential of nuclei and electrons, and $V_{xc,\sigma}$ is a local potential approximation to the exchange and correlation operators. In the present work, we have used the simple form (in Hartree a.u.)

$$V_{xc,\sigma} = -3\alpha \left(\frac{3\rho_\sigma}{4\pi}\right)^{1/3} \qquad (4)$$

with the exchange scaling constant $\alpha = 0.7$. This scheme has been found to give an accurate representation of ground state binding energies and geometries, as well as successfully predicting photoelectron energies for a

variety of molecular systems[3]. More elaborate exchange-correlation potentials such as those of Hedin and Lundqvist[10] produce relatively small changes in calculated properties, as seen for example in comparative studies on small molecules[3] and metal clusters[11].

A further problem in applying LD theory to the study of hyperfine fields, is the presence of correlation effects which are rather crudely treated by configuration averaging. For example, in the dimer Fe_2 there exist a large number of low lying multiplets, resulting from various coupling arrangements within the incomplete 3d shells of the atoms. The usual LD scheme appears to fare badly here, failing to define the ground state with sufficient precision, and yielding poor binding energies[12]. However, by applying constraints to the orbital occupation numbers $f_{n\sigma}$ one can identify the important configurations, and correlate the derived hyperfine fields with experiment[13]. A combination of LD methods with a more or less explicit treatment of a limited set of electron-electron correlations appears to be a promising line of development. The results presented in the following sections are intended to contribute toward this development, by providing a well defined measure of the predictions of the single configuration LD model.

B. Computational Method

We have made use of the Discrete Variational Method (DV-Xα), in which the molecular eigenfunctions are expanded in a linear combination of basis functions[14],

$$\psi_{n\sigma} = \sum_j \chi_j (\vec{r}) C_{jn\sigma} \qquad (5)$$

In the present work the basis $\{\chi_j\}$ has been chosen to be numerical solutions of the free atom or ion problem. The basis atoms are placed in potential wells to induce additional bound states to obtain further variational freedom.

The familiar secular matrix equation $(\underline{\underline{H}} - E\underline{\underline{S}})\,\underline{\underline{C}}$ is solved with matrix elements obtained by numerical sampling on a discrete point grid in $\vec{r}$-space. Details of this procedure have been given in previous publications[14-16], and need not be repeated here.

Since the LD theory is oriented toward determining the electronic density of the ground state, we may expect that multipolar moments and other properties of the densities ρ_σ should be well determined. Thus there is reason for some optimism about prospects for predicting contact hyperfine fields, electric field gradients (EFG), and magnetic hyperfine tensors with LD models. However, the approach is also <u>energy</u> oriented, in that the Schrödinger Eqn. (1) is solved approximately, and usually in an energy-minimization procedure. Procedures which find a minimum in the average energy, need not produce densities which are highly accurate in the vicinity of a particular probe nucleus. For this reason, it is difficult to evaluate the absoulte accuracy which is obtainable for hyperfine fields in the LD approach.

We have investigated the sensitivity of the EFG to approximations in the molecular potential, and other computational factors, for the MX_2 metal halides. The simplest approximation used, the self-consistent-charge (SCC) scheme,[16] consists of replacing the true electronic charge density $\rho(\vec{r})$ by a model density

$$\rho_{SCC}(\vec{r}) = \sum_{\nu n\ell} f^{\nu}_{n\ell} |R^{\nu}_{n\ell}(r_\nu)|^2 \qquad (6)$$

for the purpose of calculating the potential. Here $|R^{\nu}_{\ell}|^2$ are the radial densities arising from the variational basis set and the amplitudes of $f^{\nu}_{n\ell}$ are determined as Mulliken-type atomic orbital populations[17,18] obtained from the self-consistent molecular eigenvectors (c.f. Eqn. 5). This scheme has the merit of simplicity and speed, allowing an interpretation of the results in

familar chemical terms. Since ρ_{SCC} is a superposition of spherical atomic-like densities, the effects of anisotropic bonding charge tend to be somewhat reduced and averaged out. In this respect it is not very different from the muffin-tin spherical approximation used in multiple-scattering models[19-20]. As we shall see, this averaging process has a serious effect on the EFG and hence properties sensitive to charge anisotropy.

A natural extension of the SCC scheme, called the self-consistent-multipolar (SCM) expansion can be made as precise as one wishes[14,21] at additional computational cost. Here the model density is represented as

$$\rho_{SCM}(\vec{r}) = \sum_{\nu LM} \rho^{\nu}_{LM}(r_\nu)\, Y_{LM}(\hat{r}_\nu) \qquad (7)$$

where the radial densities ρ^{ν}_{LM} are associated with specific atomic sites ν and angular momentum (LM). The radial densities are determined by a least-squares fit on a sampling grid to the true molecular density, and convergence of properties with the size of the expansion is monitored. Energy eigenvalues for the MX_2 molecules studied here were observed to be rather insensitive to the addition of dipolar and quadrupolar (L=1,2) potentials; however, significant changes in the EFG were observed for the covalent-bonded iron compounds.

The EFG tensor is defined in terms of the electrostatic potential seen by the probe nucleus, as $E_{ij} = \frac{\partial E_j}{\partial X_i} = \frac{-\partial^2 V}{\partial X_i \partial X_j} = -V_{ij}$[22]. For a linear molecule, oriented along the z-axis, only the component V_{zz} is nonzero, having the value

$$V_{zz} = \sum_{\nu} Q_\nu \frac{(3z_\nu^2 - r_\nu^2)}{r_\nu^5} - \sum_{n,\sigma} f_{n,\sigma} \langle \psi_{n\sigma} | \frac{3z^2 - r^2}{r^5} | \psi_{n\sigma} \rangle. \qquad (8)$$

Here the first sum refers to nuclei with charge Q_ν and the second sum runs over all electron orbitals, with occupation numbers $f_{n\sigma}$. The corresponding

interaction energy gives a splitting of the nuclear gamma resonance Mössbauer line of a spin = 3/2 nucleus equal to

$$\Delta E_Q = \frac{1}{2} eQV_{zz} \equiv \frac{1}{2} e^2Qq \qquad (9a)$$

$$= 10.1\ Q(\text{barn})q(a_0^{-3})\ \text{mm/sec} \qquad (9b)$$

III. RESULTS FOR HCl AND Cl_2

In order to develop a quantitative calibration of the local density predictions for hyperfine structure (hfs) parameters relative to experiment and other theories, we must begin with the simplest systems. From atomic beam hfs experiments the quadrupole coupling constant e^2Qq/h of ^{35}Cl is known to be 109.74 MHz[23]. In order to separate the e^2Qq product into the nuclear moment Q and the electric field gradient q one resorts to theoretical calculations. A standard procedure has been to obtain q from atomic calculations of the restricted HF type, with either analytic or numerical procedures for solving the Schrödinger equation. The results do however depend noticeably on the model chosen, as measured by the matrix element $\langle r^{-3}\rangle_{3p}$. Thus Desclaux finds 6.769 a_0^{-3} in a nonrelativistic HF calculation, and 6.791 for the corresponding relativistic Dirac Fock model,[24] while Lindgren and Rosén find values of 6.682 for restricted HF and 7.596 for "optimized Hartree-Fock-Slater" models[25]. The particular HFS model which we have taken in the present work leads to a value of $\langle r^{-3}\rangle_{3p} = 7.824 a_0^{-3}$ with the corresponding q-value of 6.26 a.u.

It is therefore important to note at the outset, that the underlying theories, <u>at the atomic level</u>, differ in their predictions of q by 10-15%, with the corresponding uncertainty in deduced values of the nuclear moment. These differences arise from small, and fairly subtle shifts in the self-consistent radial density, as shown for the Cl 3p shell in Fig. 1. The well-known contraction of HF valence densities compared to HFS is easily seen. However, the core region variation dominates even the Cl 3p matrix element, causing the $\langle r^{-3}\rangle_{3p}$ HFS value to be substantially larger than that of the HF model. In all these calculations the Sternheimer shielding factors due to inner shell polarization[26] have been ignored, and correlation effects have

been crudely averaged (and partially omitted) in the self-consistent field procedure. While more elaborate theories can be and have been applied to atoms, the HF and HFS atomic results form a useful and valid reference point for comparison with molecular and solid state calculations.

For the calculation of the EFG in a diatomic molecule as well as in a polyatomic system, some care has to be taken in evaluation of the required $\langle r^{-3} \rangle$ matrix elements. To obtain satisfactory precision with a reasonable number of integration points we calculate the matrix element as the sum of three terms:

i) the one-center part, evaluated precisely using the atomic $\langle r^{-3} \rangle$ integrals and eigenvector coefficients;

(ii) multicenter contributions within a sphere of radius R_0 about the probe nucleus, evaluated by a systematic polynomial integration;[27] and

(iii) multicenter contributions to the exterior region, evaluated by the quasi-random diophantine integration method[14-16]. This procedure was found to give quite satisfactory results with a few thousand total integration points.

The fundamental limitation on precision of the theoretical EFG turns out to be eigenvector "noise"; i.e. the limited number of digits of precision obtained in eigenvectors based upon the energy-variational procedure. Thus, while energies ε_i were determined within 0.01 eV with a few thousand sampling points, it required up to 60,000 sampling points to stabilize the calculated EFG within 2%. The dominant errors were found to arise from spurious core-polarization terms, where small differences in, say, σ versus π eigenvectors, were greatly magnified by the large $\langle r^{-3} \rangle$ values. These core-level accuracy problems can be greatly reduced by adopting special integration grids, and successful applications were reported for linear $[Au(CN)_2]^{-1}$ systems[28].

Returning to HCℓ, we also investigated the role of basis set completeness

in determining the EFG, since previous HF studies had revealed a considerable sensitivity[29-32]. It appears that in this case, a numerical minimal free atom basis H° 1s; Cl° 1s, 2s, 2p, 3s, 3p is rather good, since augmenting this basis by chlorine 3d, 4s, 4p states produces only 2% changes in the EFG.

Accurate experimental data are available for HCl[33] and a careful theoretical analysis has been given by Grabenstetter and Whitehead[29], among others[30-31]. They find the importance of the Cl 1s shell to be small, but that the second shell (2s, 2p) is responsible for ~15% of the total electronic contribution. Accurate calculations reported for this simple molecule permit a determination of HF (or near HF limit) predictions, which can be related to the atomic models. The experimental value for e^2Qq/h is 67.619 MHz, and using the standard value of $Q_{Cl} = 7.984 \times 10^{-26}$ cm^2, one obtains a field gradient (unsigned) of 3.604 a.u. Subtracting the proton contribution of 0.143 a.u. leads to an experimental electronic value of $q_e = 3.46$ a.u.. Our results give $q_e = 3.20 \pm 0.03$ a.u. which is about 8% too low. If we in addition use the atomic Cl calculation and experiment to determine a value for Q_{Cl}, the discrepancy is increased to ~17%. The most extensive HF calculations are in very good agreement with experiment.

In solid Cl_2, the experimental value of e^2Qq/h is 108.5 MHz[34], leading to an experimental q of 5.68 a.u. Subtracting the nuclear contribution of 0.64 a.u. gives the electronic contribution $q_e = 5.04$ a.u. Calculations made at the equilibrium distance for Cl_2 with varying numbers of sampling points and minimal, as well as extended bases yields our theoretical estimate of $q_e = 5.24 \pm 0.02$ a.u. This value is about 3% too large. If we again use the atomic calculations to redetermine Q_{Cl} (7.328×10^{-26} cm^2 versus the literature value of 7.984×10^{-26} cm^2), then our result for Cl_2 is about 6% too low. These values may be compared with the HF results of Straub and

McLean[31] of q_e = 5.94 a.u. and values of 4.68 - 4.81 a.u. inferred from semiempircal CNDO and INDO calculations of Weber et al.[35] Thus we see that local density HFS calculations of the EFG appear to have an absolute accuracy of perhaps ± 15%, comparing favorably to alternative theoretical approaches.

IV. RESULTS FOR $FeCl_2$ AND $FeBr_2$

A. Energy Levels

The gas phase photoelectron spectra of $FeCl_2$ and $FeBr_2$ have been measured by Berkowitz et al.[36] in a study of MX_2 high temperature vapors. They also presented theoretical binding energies calculated in the $X_{\alpha\beta}$ multiple-scattering cellular model[37]. By comparison of spin-restricted and spin-unrestricted level schemes with experiment, the authors conclude that the high-spin, M_S=2 configuration is the ground state. Their results and our spin-unrestricted DV-$X\alpha$ binding energy estimates are given in Table 1. First we note that relaxation effects are quite important in the rather localized levels containing significant Fe 3d character. The overall average difference between ground state and transition state eigenvalues, which include relaxation effects, is 3.5-3.9 eV; however, in the $\delta_{g\downarrow}$ singly occupied minority spin state the shift is 4.6 eV.

The two spin-unrestricted models agree as to level ordering and the general numerical agreement as to energy and spin-splittings is reasonable, considering the differences in the two approaches. The comparison to the experimental peak positions is also fairly good, although both calculations under-estimate the first ionization potential by ~1eV. Although basis set truncation and other numerical limitations may have an effect on the calculated values, we believe this discrepancy is an indication of the importance of ↑↓ correlation effects not included in the X_α or $X_{\alpha\beta}$ models. Indeed, level shifts of ~1eV produced by the exchange and correlation potential model of von Barth and Hedin[38] have been found necessary to obtain quantitative agreement with photoelectron spectra of RX_3 rare-earth halide vapors[39].

B. Electric Field Gradients

Our results for the iron-site EFG in $FeCl_2$ are plotted in Fig. 2 for various bond lengths. The experimental sign of ΔE_Q is not known. If we take the value of $|\Delta E_Q|$ = 0.63 mm/sec determined by Litterst et al.[6] and the value Q = 0.156b found from atomic many-body calculations,[40] we can find an "experimental" value of $q_{exp} = \pm$ 0.41 a.u.. Duff et al. calculated a value for q of + 0.75 a.u. and on this basis suggested a reduction in the accepted value of $Q(^{57}Fe)$ to 0.082b.[7]. The present LD calculations predict that q(R) is positive, ~ + 1 in value at large distances and decreases steadily with R_{Fe-Cl}. The simple SCC potential leads to a rather small q-value for $R \simeq 4.1$, the gas phase equilibrium distance[41]. While some bond-length relaxation may take place in the rare gas host matrix used in the Mössbauer experiments, large changes would be required to bring the SCC q-value in agreement with q_{exp}.

Curves B and C were calculated with the more accurate SCM potential having L < 2 on the iron site and L < 1 on the Cl sites. While the SCC and SCM results are qualitatively similar, the SCM curve is shifted toward negative q-values and displays a steeper slope. Curves B and C differ in the treatment of core polarization: in curve B the core contribution (which is almost entirely due to the Fe 3s, p orbitals) is treated in the SCC model, using an accurate cylindrical-coordinate variational 26,200 integration point scheme[28]. The SCC spherical averaging does, however, lead to an incorrect (spherical atom) limit as $R \to \infty$. In curve C the core contribution is treated in the SCM model with 7200 diophantine integration points [21]. While numerical noise is certainly greater, the SCM scheme does have the correct dissociation limit; i.e. the Sternheimer shielding factor will be recovered, in principle, at large R. The deviation between curves B and C is thus a relatively good measure of computational "error-bars", and displays the importance of the Fe3p

polarization effect, as pointed out by Duff et al.[7].

In any case, the LD theory results suggest:

(i) $q < 0$;

(ii) SCC approximation, and by implication, all other spherical averaging or muffin-tin procedures is seen to be inadequate for predicting EFG in anisotropic covalent systems;

(iii) Curve B is in accidentally perfect agreement with experiment, for an assumed R = 4.1 a.u. and $q_{exp} < 0$. This is our best estimate from the point of view of numerical stability. Curve C suggests that somewhat reduced values of $|Q_{Fe}|$ be considered;

(iv) our results are inconsistent with the HF calculations of Duff et al. with respect to sign of q.

There are several further possibilities to consider:

(i) The Fe-Cℓ bond length may change in the crystal. A contraction would be expected due to packing forces exerted by the closed shell atoms of the lattice. However, the rare-gas matrix could also induce chemical changes in the Fe-Cℓ bond. The existence of stable species like XeF_6 and KrF_2 shows that there is indeed a bonding interaction between rare-gas and halogen atoms. Theoretical investigation of this possibility would require treatment of clusters like $FeCℓ_2Ar_4$ and $FeCℓ_2Ar_{12}$ which are beyond the scope of the present work.

(ii) The "monomer" peak is the Mössbauer spectra may be misidentified. For example, in argon-isolated $FeCℓ_2$ there are also peaks at 1.79 and 2.80 mm/sec attributed to dimers and bridge-bonded dimers, respectively[5,6] and rather close to that found (1.30 mm/sec) for crystalline $FeCl_2$.

We tend to suspect item (i) is relevant, and have some hopes of carrying out the larger cluster studies in the future. At the present, it would be

extremely helpful to obtain new experimental data, namely, a direct measurement of R(Fe-Cℓ) by EXAFS techniques, and a determination of the sign of the EFG, requiring the use of a magnetic field in Mössbauer measurements. We may see such data in the near future[42].

In order to gain an understanding of the rapid variation of the EFG with bond length, we have performed a detailed orbital analysis at each R. The majority spin ↑ and minority spin ↓ valence orbitals have quite different V_{zz} values, due to the four unbalanced spins and the resulting distortion of the occupied state wavefunctions. The total spin ↑ valence contribution is negative and grows steadily in magnitude as R decreases, due largely to bonding effects in the unpaired $9\sigma_g$, $3\pi_g$ levels. The spin ↓ valence contribution is however positive for R > 4.0 a.u., becoming steadily smaller as R decreases. This reduction (also present in spin ↑) can be largely traced to a contraction of the doubly occupied $6\sigma_u$,$7\sigma_u$ states at smaller distance -essentially an overlap repulsion effect. The result is that V_{zz} decreases steadily with R. Two-and three center contributions of either spin are negative, and essentially cancel against nuclear terms for large R values. The multicenter contribution grows rapidly as R decreases, reaching ~130% of the bare nucleus value for R=4.1 a.u. and is thus a significant contributor to the EFG.

The Fe 1s, 2s,2p shells are found to contribute only negligibly to the EFG; apparently they are well shielded by the rather polarizable 3s, 3p shells. The 3s, 3p "semicore" terms are positive and also grow rapidly as R decreases, reaching 23% of the off-site nuclear dipolar terms at R=4.1 a.u. Written as a Sternheimer shielding factor,

$$V_{zz,tot} = (1-R_s)V_{zz,valence} + V_{zz,off\text{-}site} \qquad (10)$$

We find $R_S \cong 0.48$ at this distance.

Since the effective R_S is determined by the self-consistent interaction of all electrons and nuclei, and is rapidly varying with R (it becomes negative at small R values), estimates based upon simplified free ion models may not be reliable.

Now let us briefly summarize our EFG results for $FeBr_2$, which lead to very similar conclusions to those reached for the chloride. Assuming again the nuclear moment Q(Fe) = 0.156b, the "monomer peak" of Litterst et al.[6] for $FeBr_2$ in an argon matrix leads to a value $|q_{exp}| = 0.56$ a.u., which is ~40% greater than in $FeCl_2$. The HF value of Duff et al.[7], calculated at the gas phase bond length R(FeBr) = 4.36 a.u. is $q_{HF} = +1.09$ a.u. again leading them to suggest a reduction of the accepted value of Q(Fe) by nearly a factor of two. Our calculations of q(R) using the SCC approximation to the potential give an asymptotic value of ~ + 1 a.u. at large R. For any reasonable range of R-values, $4.2 < R < 4.5$ a.u., the absolute value |q| is too small, compared to experiment. The more accurate SCM potential shifts the q(R) curve down toward more negative values as in $FeCl_2$. We definitely predict $q < 0$, and in our best estimate, a bond contraction of ~0.15 a.u. would match experiment and theory (assuming Q = 0.156b).

C. Magentic Hyperfine Fields and Isomer Shifts

The magnetic hyperfine field at the iron nucleus due to the unpaired electronic spin density is:

$$B_{hf} = 524.2\rho_s(0) \text{ kG} \qquad (11)$$

with ρ_s given in e/a_0^3 units. Since only $\ell = 0$ densities have nonzero value at the origin, the observable contact field is the result of polarization of the Fe 1s, 2s, 3s, 4s shells by the unpaired 3d-electrons, in the case of the free ion, and for the coresponding molecular orbitals in the case of FeX_2

molecules.

The net field is found to be negative in both $FeCl_2$, and $FeBr_2$, consistent with observations on many other systems.

$$B_{hf} = -432kG \text{ at } R = 4.1\ a_0 \text{ for } FeCl_2, \text{ and}$$

$$B_{hf} = -468kG \text{ at } R = 4.36\ a_0 \text{ for } FeBr_2 .$$

The required core-polarization terms were calculated using a relativistic moment-polarized free ion model[45] with the configuration found from the self-consistent molecular results. The $2s_{1/2}$ contribution dominates the core contribution, which is -1617kG in total. Contributions of 3s and 4s levels are found to be positive in the free ion as well as in the FeX_2 molecule. However, due to differential mixing with π,ϕ ligand orbitals the MO valence contributions are nearly three times as large as in the free ion.

The isomer shifts (IS) of the Mössbauer nuclear gamma resonance is given by

$$\Delta E_{IS} = a\Delta\rho_c(0) \text{ mm/sec} \qquad (12)$$

where $\Delta\rho_c$ (0) is the difference in electronic charge density at the iron nucleus between some reference system and the measured system. A current estimate of the IS calibration constant is[46] $a = -0.27 \text{ (mm/sec)}/(e/a_0)^3$.

Litterst et al. report IS values of +0.88 and +0.81 ± 0.02 mm/s for $FeCl_2$ and $FeBr_2$ in argon matrices, respectively[6]. The IS values are given relative to metallic iron at 300K. The absolute values of $\rho_c(0)$ calculated in our variational molecular procedure are not very accurate; however, differences $\Delta\rho_c(0)$ can be determined reliably. We find an increase, $\Delta\rho_c = +0.18\ e/a_0^3$, in passing from $FeCl_2$ to $FeBr_2$ at the supposed equilibrium

distances. This value is consistent in sign and approximate magnitude with the observed IS difference. This result can be taken as an argument that bond lengths are not much changed in the host lattice, since we find a rate of change $\partial\rho_c/\partial R = -1.6\ e/a_0^4$ around the assumed equilibrium position.

D. Halogen Quadrupole Coupling Constants

The quadrupole coupling constant for the halogen site in FeX_2 is measurable, in principle, by NMR techniques. The ^{35}Cl e^2Qq/h value in solid $FeCl_2$ has been found to be 4.74 MHz[43], but will be expected to be quite different in the layered compound, compared to the matrix-isolated molecule. We have calculated the EFG at the chlorine site in $FeCl_2$ and at the bromine site in $FeBr_2$ for several values of R(Fe-X) around the equilibrium distance. The value of q is positive in both cases, increasing in magnitude with R. Inner-shell polarization is found to give a shielding effect of ~5%, which is appreciably smaller than that of the Fe-site. The theoretical values found are $q(Cl) = +1.88 \pm 0.1\ a_0^{-3}$ at $R = 4.1\ a_0$, and

$q(Br) = +3.25 \pm 0.1\ a_0^{-3}$ at $R = 4.36 a_0$.

For chlorine, this result leads to a predicted e^2Qq/h value of ~22.1 MHz, about 20% of experimental value of Cl_2.

V. RESULTS FOR $EuCl_2$

The rare-earth halides form an interesting contrast to their transition metal counterparts, since the partially occupied 4f shell is more localized and presumably not directly involved in the M-X bond. Mössbauer absorption spectra have been obtained for matrix isolated $EuCl_2$, and interpreted on the basis of a 6s-6p hybridization model[8,9]. The effective ionicity obtained in this work is 0.47, corresponding to a configuration Eu $4f^7$ $6s^{0.53}$ $6p^{0.53}$ quite different from the nominal Eu^{2+}, Cl^- states corresponding to purely ionic bonding.

We have calculated the self-consistent energy levels and charge and spin densities for $EuCl_2$, as a function of internuclear separation. The results show that the $(4f\uparrow)^7$ fully polarized state of europium is favored in this linear molecule, in analogy with the $(3d\uparrow)^5$ $(3d\downarrow)^1$ high spin state found in $FeCl_2$ and $FeBr_2$. Ground state eigenvalues corresponding to a bond length R(Eu-Cl) = 5.5 a.u., near the estimated equilibrium value, are given in Table 2. The exchange splitting of the Eu-f levels is seen to be ~5eV, and these states are very little mixed with ligand character. The identification of the high spin state as the ground configuration implies a magnetic hyperfine field B_{hf} of the order of 300kG, as measured in EuS and many other compounds[22]. In cubic systems, B_{hf} leads to a set of resolved Mössbauer lines corresponding to an overlay of many transitions from the I=7/2 excited state to the I=5/2 ^{151}Eu nuclear ground state. The typical width of the spectrum is ~40 mm/sec.

The data of Baggio-Saitovitch et al. shows a rather broad unresolved spectrum, which was interpreted in terms of an isomer shift of -13.4 mm/s (relative to $^{151}Sm_2O_3$) and a quadrupole interaction e^2Qq/h = -235 MHz[8,9]. Magnetic hyperfine interactions were assumed to be absent.

Theoretical q-values of the Eu-site in $EuCl_2$ are plotted versus R in Fig.3.

Because of the simple bonding scheme in this molecule, we find the theoretical results to be very insensitive to computational details such as choice of basis, multipolar components of potential, number of integration points, etc. We see from Fig. 3 that the predicted EFG is much larger, though of the same sign, as that inferred from experiment. Here (in contrast to $FeCl_2$) the experimental sign of the EFG is known, and we have used the value Q = 1.14 b[44]. The variation of q with R is seen to be more rapid than R^{-3}; this shows that while the bonding is ionic the effective charge carried predominantly by the Eu 5d, 6s, 6p shells is itself a rapidly changing function of R. At a distance R = 5.5 a.u., using a small but partially optimized numerical basis set, we find the effective configuration $Eu^{+1.31}$ $4f^7$ $5d^{0.43}$ $6s^{0.11}$ $6p^{0.15}$. Numerical integration of the spatial volume nearest to the Eu-site yields a net charge of +1.40 which is quite consistent with the Mulliken atomic charge of +1.31.

The calculations reported here are carried out in a nonrelativistic framework. While relativistic corrections may turn out to be sizable, it is very unlikely that they are large enough to change our main conclusions, which are:

i. The high-spin state is the ground state of $EuCl_2$, and hence a sizable magnetic hyperfine field is present.

ii. In addition to the 6s, 6p hybridization previously proposed to account for the bonding, we find a sizable Eu 5d bonding component, which makes significant contributions to the Eu-site EFG.

iii. A large discrepancy between q_{expt} and q_{theory} is noted, which could readily be attributed to the neglect of 5d-bonding effects and the presence of a magnetic hyperfine field in analysis of the experimental data. It would be interesting to attempt a reinterpretation of the Mössbauer data in light of these results, especially if the equilibrium R-value can be determined by EXAFS or other techniques.

ACKnOWLEDGEMENTS

This research was supported in part by the NSF, Grant no. DMR82-14966, by the Conselho Nacional de Desenvolvimento Cientifico e Technologico (Brasil), and by NATO, Grant No. 1826. HBJ thanks the Netherlands-America Foundation for fellowship support.

REFERENCES

1. J.C. Slater, The Self-Consistent Field For Molecules and Solids, (McGraw-Hill, New York, 1974).
2. V.L. Moruzzi, J.F. Janak and A.R. Williams, Calculated Electronic Properties of Metals, (Pergamon, New York, 1978).
3. E.J. Baerends and P. Ros, Int. J. Quantum Chem. Symp 12, 169, (1978).
4. W. Kohn and L.J. Sham, Phys. Rev. 140, A1133 (1965).
5. T.K. McNab, D.H.W. Carstens, D.M. Gruen and R.L. McBeth, Chem. Phys. Lett. 13, 600 (1972).
6. F.J. Litterst, A. Schichl and G.M. Kalvius, Chem. Phys. 28, 89 (1978).
7. K.J. Duff, K.S. Mishra and T.P. Das, Phys. Rev. Letters 46, 1611 (1981).
8. E. Baggio - Saitovitch, F.J. Litterst and H. Micklitz, J. de Phys. 37, C6-529 (1976).
9. F.J. Litterst, A. Schichl, E. Baggio - Saitovitch, H. Micklitz and J.M. Friedt, Ber. Bunsenges, Phys. Chem. 82, 73 (1978).
10. L. Hedin and B.I. Lundqvist, J. Phys. C4, 2064 (1971); O. Gunnarson and and B.I. Lundqvist, Phys. Rev. B13, 4274 (1976).
11. B. Delley, D.E. Ellis, A.J. Freeman, E.J. Baerends and D. Post, Phys. Rev. B (to be published).
12. J. Harris and R.O.Jones, J. Chem. Phys. 70, 830 (1979); B. Delley (private communication).
13. D. Guenzburger and E.M. Baggio - Saitovitch, Phys. Rev. B24, 2368 (1981).
14. D.E. Ellis and G.S. Painter, Phys. Rev. B2, 2887 (1970); E.J. Baerends, D.E. Ellis and P. Ros, Chem. Phys. 2, 41 (1973).
15. D.E. Ellis and F.W. Averill, J. Chem. Phys. 60, 2856 (1974).
16. A. Rosén, D.E. Ellis, H. Adachi and F.W. Averill, J. Chem. Phys. 85, 3629 (1976).

REFERENCES (CONTINUED)

17. R.S. Mulliken, J. Chem. Phys. 23, 1833 (1955).

18. C. Umrigar and D.E. Ellis, Phys. Rev. B21, 852 (1980).

19. J.C. Slater and K.H. Johnson, Phys. Rev. B5, 844 (1972); J.C. Slater, Adv. Quant. Chem. 6, 1 (1972); K.H. Johnson, Adv. Quant. Chem. 7, 143 (1973).

20. N. Rösch, in Electrons in Finite and Infinite Structures, ed. by P. Phariseau (Plenum, New York, 1977).

21. B. Delley and D.E. Ellis, J. Chem. Phys. 76, 1949 (1982).

22. For example see N. N. Greenwood and T.C. Gibb, Mössbauer Spectroscopy, (Chapman and Hall, London, 1971) where applications to nuclear gamma ray resonance are worked out in detail.

23. V.Jaccarino and J.G. King, Phys. Rev. 63, 471 (1955).

24. J.P. Desclaux, At. Data and Nucl. Data Tables 12, 311 (1973).

25. I. Lindgren and A. Rosén, Case Studies in At. Phys. 4, 197 (1974).

26. R.M. Sternheimer, Phys. Rev. 80, 102 (1950); K.D. Sen and P.T. Narasinhan, Phys. Rev. B16, 107 (1977) and references therein.

27. A.H. Stroud, Approximate Calculation of Multiple Integrals, (Prentice-Hall, Englewood Cliffs, N.J. 1971).

28. D. Guenzburger and D.E. Ellis, Phys. Rev. B22, 4203 (1980).

29. J.E. Grabenstetter and M.A. Whitehead, J.C.S. Faraday II-1 (1978); ibid, Chem. Phys. Lett. 37, 547 (1976); Can. J. Chem. 54, 1948 (1976); S. Engström and H. Wennerström, Mol.Phys. 36, 773 (1978).

30. R. Moccia, Theor. Chim. Acta 8, 8 (1967).

31. A.D. McLean and M. Yoshimine, J. Chem. Phys. 47, 3256 (1967); P.A. Straub and A.D. McLean, Theoret. Chim. Acta (Berl.) 32, 227 (1974).

32. M-C Montabonel, M. Suard and L. Guibe, Mol. Phys. 40, 1503 (1980).

33. E.W. Kaiser, J. Chem. Phys. 53, 1686 (1970).

REFERENCES (CONTINUED)

34. N. Nakamura and H. Chihara, J. Phys. Soc. Japan 22, 201 (1967).

35. J. Weber, V.A. Gubanov and A.A.V. Gibson, J. Magn. Res. 20, 427 (1975); S. Sengupta, G. Litzistorf and E.A.C. Lucken, J. Magn. Res. 41, 169 (1980); A. Coker, T. Lee and T.P. Das, J. Chem. Phys. 66, 3903 (1977).

36. J. Berkowitz, D.G. Streets and A. Garritz, J. Chem. Phys. 70, 1305 (1979).

37. J. Keller, Intern. J. Quantum Chem. 9, 583 (1975); F. Herman, J. van Dyke and I.B. Ortenburger, Phys. Rev. Letters 22, 807 (1969).

38. U. von Barth and L.Hedin, J. Phys. C5, 1629 (1972).

39. B. Ruščić, G.L. Goodman and J. Berkowitz (to be published).

40. S.N. Ray and T.P. Das, Phys. Rev. B16, 4794 (1977).

41. E. Vajda, J. Tremmel and I. Hargittai, J. Mol. Struc. 44, 101 (1978).

42. P.A. Montano and G.K. Shenoy (private communication).

43. R.G. Barnes and S.L. Segel, J. Chem. Phys. 37, 1895 (1962).

44. Mössbauer Effect Data Index, eds. J.G. Stevens and V.E. Stevens (Plenum, New York, 1975).

45. D.E. Ellis, J. Phys. B10, 1 (1977); ibid, Intern. J. Quantum Chem. Symp. 11, 201 (1977).

46. D. Guenzburger, D.M.S. Esquivel, and J. Danon, Phys. Rev. B18, 4561 (1978).

Table 1. Comparison of theoretical and experimental one electron binding energies (in eV) for $FeCl_2$ and $FeBr_2$. Arrows ↑,↓ indicate majority, minority spin state in spin-unrestricted calculations.

expt[a]		[b] ↑ $X_{\alpha\beta}$ ↓		[c] ↑ DV-X_α ↓	
$FeCl_2$					
10.45	δ_g	13.1	9.3[(d)]	11.8(11.7)	8.4(9.4)[d]
11.26	σ_g	10.8	-	10.9(11.9)	8.1
11.91	π_g	10.8	-	10.0(10.0)	8.1
12.12	π_u	11.5	11.4	10.6	10.3(10.3)
(12.53)	π_g	13.5	11.8	12.7	10.7
13.67	σ_u	12.5	12.2	11.4(11.3)	11.0
	σ_g	15.0	13.8	13.6	12.2
	σ_u			22.4	22.1
	σ_g			22.6	22.3
$FeBr_2$					
9.95	δ_g	12.6	9.1[d]	11.3	8.2[d]
10.65	σ_g	10.5	-	10.7	8.0
11.14	π_g	10.2	-	9.6	7.9
11.40	π_u	10.7	10.5	10.2	9.9
12.01	π_g	13.0	10.7	12.4	10.4
13.23	σ_u	11.6	11.3	10.9	10.5
(14+?)	σ_g	14.3	12.6	13.3	11.8
	σ_u	22.5	22.2	21.8	21.5
	σ_g	22.8	22.5	22.0	21.7

(a) Ref. 36

(b) Spin-unrestricted $X_{\alpha\beta}$ multiple scattering method, Ref. 36,37 with R=4.09 a.u. for $FeCl_2$ and R=4.39 a.u. for $FeBr_2$

(c) Present work, R=4.2 a.u. for $FeCl_2$ and R=4.36 for $FeBr_2$. Levels in parentheses are separately optimized transition state values; remainder are ground state levels shifted by 3.6 eV.

(d) Highest occupied level.

Table 2. Self-consistent spin-polarized ground state energy levels (in eV) for $EuCl_2$, at bond length R=5.5 a.u.. Levels predominantly of Eu 4f character are indicated.

Level	spin ↑	↓
π_u	4.2[a]	4.3
$\phi_u(f)$	6.6	0.9[b]
π_g	4.4	4.4
$\sigma_u(f)$	6.5	0.6[b]
σ_u	4.5	4.5
σ_g	5.3	5.2
$\pi_u(f)$	6.4	0.6[b]
$\delta_u(f)$	6.5	0.7[b]
σ_u	15.6	15.6
σ_g	15.7	15.8
σ_u	22.7	20.1
π_u	23.1	20.5

(a) Last occupied level.

(b) Empty level.

Figure Captions

1. Difference in electron density of the atomic Cℓ 3p orbital between HF and HFS theories. The maximum in the density itself is about 0.25 a.u. and is reached at R = 1.5 a.u.
2. Calculated values of electric field gradient parameter q at the Fe site in $FeCℓ_2$ plotted against Fe-Cℓ distance. Curve (a) represents values from a SCC calculation using 26200 integration points in a cylindrical coordinate mesh. Curve (b) represents a SCM calculation ($L < 2$) with 7200 points in a diophantine integration scheme. Fe 1s,2s,2p,3s,3p core contributions to q were obtained in the same manner as curve (a). Curve (c) represents an SCM calculation with all electrons treated by the diophantine integration scheme. Point (d) is a single calculation done in the same manner as (c), with 14400 points to test integration convergence. Points (e) represent the value inferred from experiment (Ref. 6) for which the sign is undetermined. ($|V_{zz}| = 0.41$ a.u.). Point (f) is the theoretical value calculated by Duff et al. (Ref. 7).
3. Calculated values of electric field gradient parameter q at Eu site in EuCℓ plotted against Eu-Cℓ distance. Curve (a) is $-(6/R)^3$, representing a simple point-ion model. Curve (b) represents an SCM calculation ($L < 2$). The "experimental" value of $q = -0.86$ a.u. inferred from Refs. (8,9) is indicated by brackets.

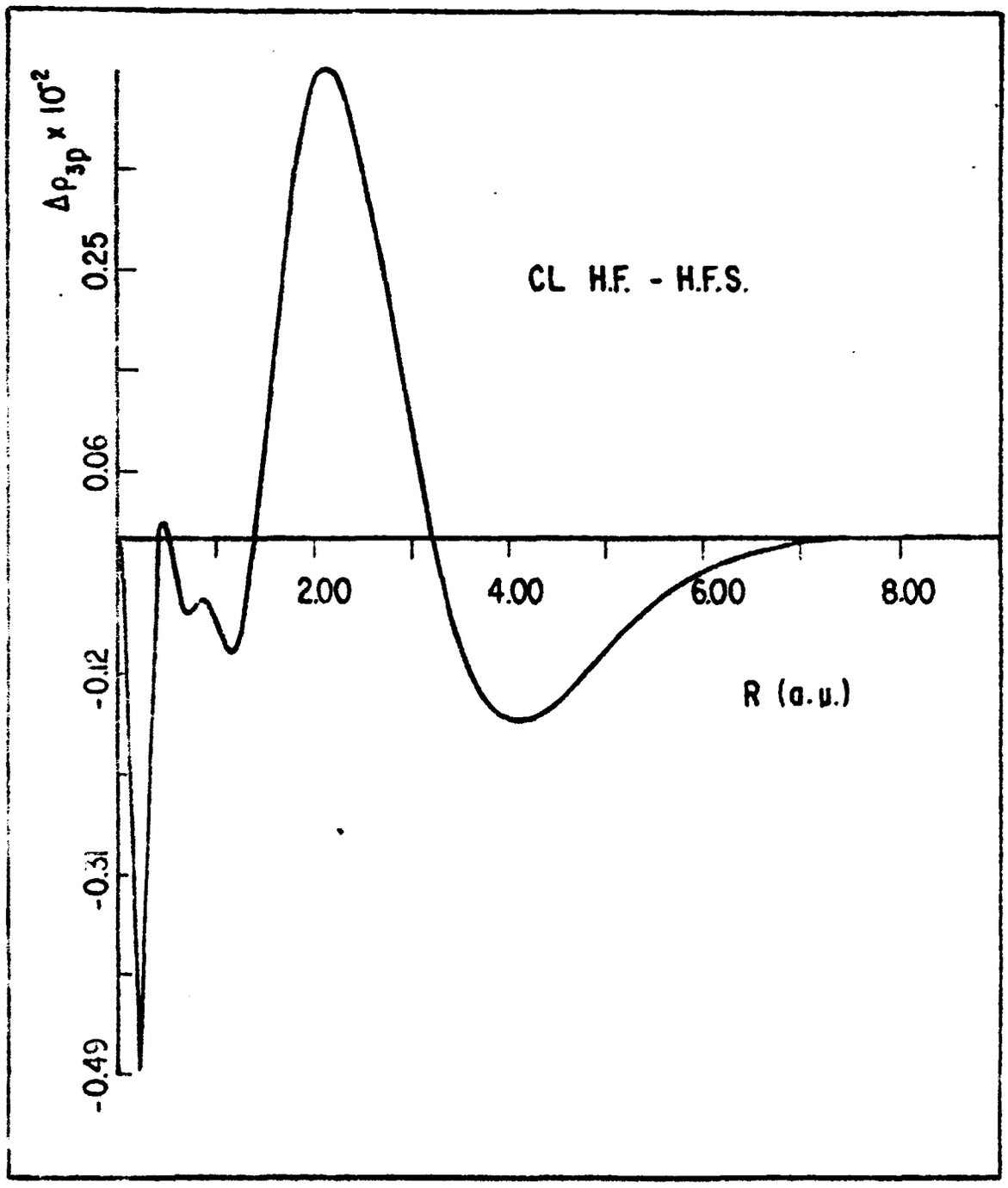
$\Delta\rho_{3p} \times 10^2$
0.25
0.06
-0.12
-0.31
-0.49
CL H.F. - H.F.S.
2.00
4.00
6.00
8.00
R (a.u.)

Fig. 1

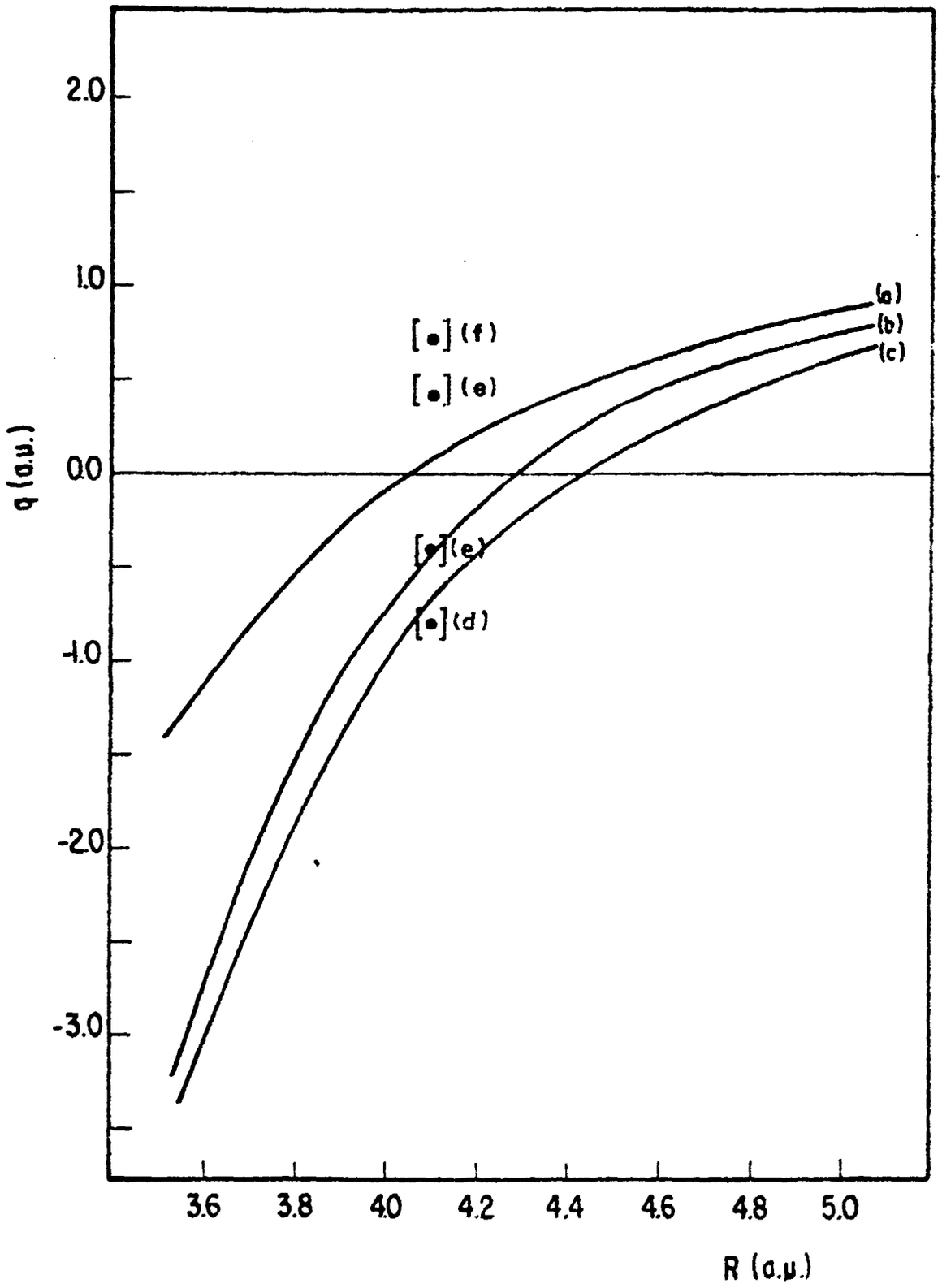

Fig. 2

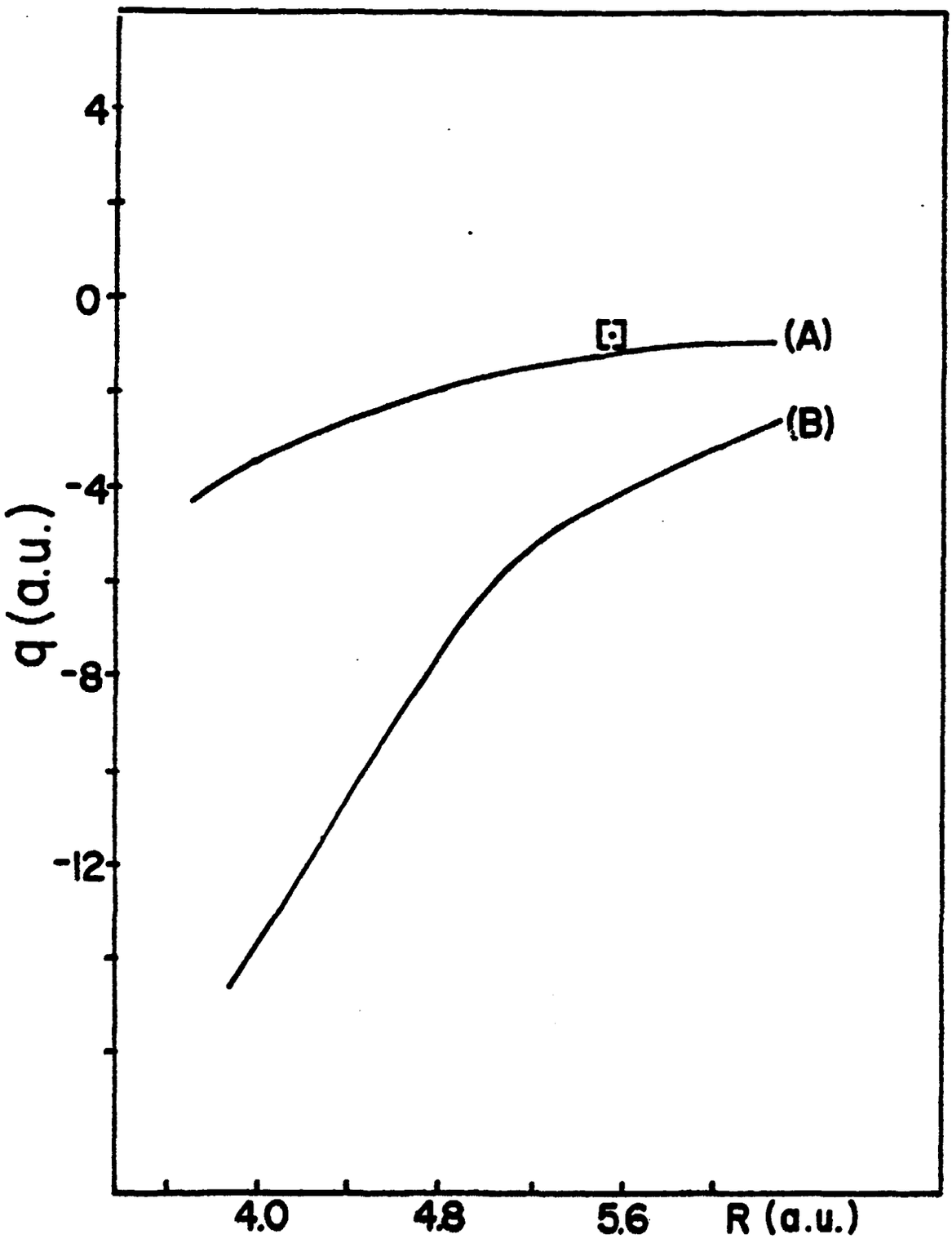

Fig. 3